



Characterization Rig for Antennas and Retroreflectors

**A Degree Thesis
Submitted to the Faculty of the
Escola Tècnica d'Enginyeria de Telecomunicació de
Barcelona
Universitat Politècnica de Catalunya
by
Ariel Trumper**

**In partial fulfilment
of the requirements for the degree in
TELECOMMUNICATIONS SYSTEMS ENGINEERING**

Advisors: Alba Pagès-Zamora, Taimur Aftab

Barcelona, January 2018

Abstract

Universal wireless sensing is expected to be a key upcoming mass application of wireless telecommunications technology. Wireless characterization of devices such as wireless sensors, motors, RFID sensing tags and passive retroreflectors is of great interest.

Several members of the Department of Microsystems Engineering (IMTEK), at the Albert-Ludwigs University of Freiburg, carry out experiments throughout the year regarding antennas and retroreflectors. The applications of these experiments are very wide, like urban search and rescue radars, microwave DRs or SAW RFID tags. This project has been developed there, that is why it is focused on their needs and possibilities.

The goal of this thesis is to develop a new antenna testing rig that can be used to measure those devices in a reliable way. The project includes several parts, such as the mechanical (building the structure for the rig), electrical (sensors and motor configuration) and software part (testing, post processing...). It includes a user manual too, which is created in order to make it possible for everyone to use the device.

The system shall be able to characterize the radiation pattern of any given antenna. Powered by a stepper motor in its base, the antenna rotates and a pattern is generated, for later processing via MATLAB.

As a result, everyone can easily use the developed equipment for their purposes in a reliable way. In the future, more features can be added to the product to make it even more versatile.

Resum

S'espera que els sensors inalàmbrics universals siguin la propera clau per a l'aplicació en massa de la tecnologia de telecomunicacions sense fils. La caracterització sense fils de dispositius tals com sensors inalàmbrics, motors, etiquetes de detecció RFID i retrorreflectors passius és de gran interès.

Diversos membres del Departament d'Enginyeria de Microsistemes (IMTEK), a la Universitat Albert-Ludwigs de Friburg, realitzen experiments durant tot l'any amb antenes i retrorreflectors. Les aplicacions d'aquests experiments són molt àmplies, com ara radars de recerca i rescat urbans, ressonadors dielèctrics de microones o etiquetes SAW RFID. Aquest projecte ha estat desenvolupat allà, i és per això que se centra en les seves necessitats i possibilitats.

L'objectiu d'aquesta tesi és desenvolupar un nou equip de prova d'antenes que pugui ser utilitzat per mesurar aquests dispositius d'una manera fiable. El projecte inclou diverses parts: la part mecànica (construcció de l'estructura per a l'equip), elèctrica (sensors i configuració del motor) i de software (proves, post-processament ...). També inclou un manual d'usuari, creat perquè tothom pugui utilitzar el dispositiu.

El sistema haurà de ser capaç de caracteritzar el diagrama de radiació de qualsevol antena donada. Impulsada per un motor pas a pas a la base, l'antena gira i es genera un diagrama de radiació, per al seu posterior processat via MATLAB.

Com a resultat, tots poden utilitzar l'equip desenvolupat per als seus propòsits d'una manera fiable. En el futur, es poden afegir més característiques al producte per fer-ho encara més versàtil.

Resumen

Se espera que los sensores inalámbricos universales sean la próxima clave para la aplicación en masa de la tecnología de telecomunicaciones sin cables. La caracterización inalámbrica de dispositivos tales como sensores inalámbricos, motores, etiquetas de detección RFID y retrorreflectores pasivos es de gran interés.

Varios miembros del Departamento de Ingeniería de Microsistemas (IMTEK), en la Universidad Albert-Ludwigs de Friburgo, realizan experimentos durante todo el año con antenas y retrorreflectores. Las aplicaciones de estos experimentos son muy amplias, tales como radares de búsqueda y rescate urbanos, resonadores dieléctricos de microondas o etiquetas SAW RFID. Este proyecto ha sido desarrollado allí, y es por lo que se centra en sus necesidades y posibilidades.

El objetivo de esta tesis es desarrollar un nuevo equipo de prueba de antenas que pueda ser utilizado para medir esos dispositivos de una manera fiable. El proyecto incluye varias partes: la parte mecánica (construcción de la estructura para el equipo), eléctrica (sensores y configuración del motor) y de software (pruebas, post-procesamiento...). También incluye un manual de usuario, creado para que todos puedan utilizar el dispositivo.

El sistema deberá ser capaz de caracterizar el diagrama de radiación de cualquier antena dada. Impulsada por un motor paso a paso en su base, la antena gira y se genera un diagrama de radiación, para su posterior procesado vía MATLAB.

Como resultado, todos pueden utilizar el equipo desarrollado para sus propósitos de una manera fiable. En el futuro, se pueden añadir más características al producto para hacerlo aún más versátil.

Acknowledgements

First of all, I would like to thank the support shown by my advisor in Freiburg, Taimur Aftab. Not only has he provided me with a lot of information and knowledge, but also dedicated a lot of his time and effort for the correct development of my Bachelor's Thesis.

Also, I would like to especially thank the technical staff of IMTEK for helping me with an essential part of my thesis, and all the things that I needed from them. I have received their help whenever I asked for it, without hesitation.

Finally, I also want to thank the rest of the staff at the IMTEK department, who welcomed me and helped me with anything I needed.

Revision history and approval record

Revision	Date	Purpose
0	20/12/2017	Document creation
1	24/01/2018	Document revision

DOCUMENT DISTRIBUTION LIST

Name	e-mail
Ariel Trumper	arieltrumper@gmail.com
Taimur Aftab	aftab@imtek.de
Alba Pagès-Zamora	alba.pages@upc.edu

Written by:		Reviewed and approved by:	
Date	25/01/2018	Date	25/01/2018
Name	Ariel Trumper	Name	Taimur Aftab
Position	Project Author	Position	Project Supervisor

Table of contents

Abstract	1
Resum	2
Resumen	3
Acknowledgements	4
Revision history and approval record	5
Table of contents	6
List of Figures	8
1. Introduction.....	10
1.1. Statement of Purpose	10
1.2. Requirements and Specifications	10
1.3. Methods and Procedures.....	11
1.4. Work Plan.....	11
1.5. Incidences and Modifications.....	12
2. State of the art of the technology used or applied in this thesis.....	13
2.1. Anechoic Chambers	13
2.1.1. <u>Radio-Absorbent Material (RAM)</u>	14
2.1.2. <u>Electromagnetic Compatibility</u>	14
2.2. Applications.....	14
2.2.1. <u>Wireless Patch Antennas</u>	14
2.2.2. <u>Chip-based RFID</u>	15
2.2.3. <u>Retroreflectors Wireless Passive Sensing</u>	16
2.2.4. <u>Urban Search and Rescue Antennas</u>	16
3. Methodology	18
3.1. Mathematical modelling	18
3.1.1. <u>Link Budget</u>	18
3.1.2. <u>Antennas</u>	18
3.1.3. <u>Friis Equation</u>	19
3.2. Software	21
3.2.1. <u>MATLAB</u>	21
3.2.2. <u>SolidWorks and Ultimaker Cura</u>	23
3.2.3. <u>LabView</u>	25
3.3. Hardware.....	25

3.3.1.	<u>Stepper motor</u>	26
3.3.2.	<u>Stand Structure</u>	27
3.4.	User Manual	28
3.4.1.	<u>Antenna Stand Set-Up</u>	28
3.4.2.	<u>Parameters Set-Up and Measurement</u>	29
4.	Results	31
4.1.	Hardware Performance	31
4.2.	Software Performance.....	32
4.2.1.	<u>Dipole Antenna</u>	32
4.2.2.	<u>Hybrid PA-23R Antenna</u>	33
4.2.3.	<u>2.4GHz Flat Antenna</u>	35
5.	Budget.....	38
6.	Conclusions and future development.....	39
7.	Bibliography.....	40
8.	Appendices.....	41
9.	Glossary	44

List of Figures

Figure 1.1: Gantt Diagram representation throughout the project: a) Work Plan diagram, b) Critical Review diagram, c) Final Report diagram	12
Figure 2.1: Anechoic chamber testing [1].....	13
Figure 2.2: Wireless interrogation of the antenna sensor based on antenna backscattering: (a) antenna impedance switching; (b) implementation of light-activated RF switching [1]	15
Figure 2.3: a) Design of the RFID chip-based touch sensor, b) inkjet printed RFID touch sensor prototype [2].....	15
Figure 2.4: Wireless temperature sensing using DR with a separately coupled antenna [3]	16
Figure 2.5: Testing set for USAR [4]	17
Figure 3.1: Two-way propagation by ground reflections from transmitter (S) to receiver (E)	20
Figure 3.2: Data extractor uninitialized.....	21
Figure 3.3: Motion control commands.....	22
Figure 3.4: Example of radiation pattern of dipole at 500MHz.....	23
Figure 3.5: a) first design of encoder holder, b) printed final piece	23
Figure 3.6: a) design of shaft holder, b) printed shaft holder	24
Figure 3.7: Ultimaker design of encoder holder.....	24
Figure 3.8: Ultimaker design of holding piece	25
Figure 3.9: a) Ultimaker design of shaft holder, b) different layers of shaft holder	25
Figure 3.10: Stepper motor parts	26
Figure 3.11: Stepper motor inside gears	27
Figure 3.12: Stand structure for stepper motor and DUT	27
Figure 3.13: DUT and antenna stand.....	28
Figure 3.14: Test set-up example, done in the RF laboratory.....	28
Figure 3.15: LabView screen for the antenna tests	29
Figure 3.16: State diagram of the LabView program	30
Figure 4.1: Final set-up for the experiments in the warehouse.....	31
Figure 4.2: Dipole antenna, 0.5-3GHz	32
Figure 4.3: Radiation patterns of dipole; a) inside frequency range, b) outside frequency range	33
Figure 4.4: V- and H-Polarization values (dB) of the dipole for different frequencies.....	33
Figure 4.5: WiMo PA-23R antenna, 1.24-1.32GHz	34
Figure 4.6: Radiation patterns of PA-23R antenna; a) and b) inside frequency range, c), d), e) and f) outside frequency range	35

Figure 4.7: V- and H-Polarization values (dB) of the PA-23R antenna for different frequencies.....	35
Figure 4.8: Flat Antenna, 2.3-2.5GHz	36
Figure 4.9: Radiation patterns of flat antenna; a) inside frequency range, b) and c) outside frequency range	36
Figure 4.10: V- and H-Polarization values (dB) of the flat antenna for different frequencies	37
Figure 8.1: Double polarized horn antenna	41
Figure 8.2: Isotropic gain for different frequencies	41
Figure 8.3: Radiation pattern for 500MHz, E-Plane and H-Plane	42
Figure 8.4: Radiation pattern for 1GHz, E-Plane and H-Plane	42
Figure 8.5: Radiation pattern for 2GHz, E-Plane and H-Plane	42
Figure 8.6: Radiation pattern for 2.5GHz, E-Plane and H-Plane	43
Figure 8.7: 3dB bandwidth at different frequencies	43

1. Introduction

1.1. Statement of Purpose

There is a need in wireless communications to characterize radiation patterns and performances of antennas installed in embedded systems. Therefore, the purpose of this project is to develop a characterization rig for antennas and retroreflectors, together with the processing software that allows to analyse the acquired data.

Some of the special applications this test rig may have are:

- Antennas for urban search and rescue (USAR)
- Retroreflectors passive sensors
- Antennas mounted on embedded systems

This thesis consists in designing and building a transportable rig for antenna testing, which includes 1 calibration antenna (dual polarized antenna BBHX 9120-E) that will be used for environmental characterization, and a second antenna that will be the device under test (DUT). The idea is to characterize the radiation pattern of the DUT and analyse the data acquired during the test. This will be possible with a software and a user's manual also developed during the project.

The project's main goals are:

- 1- Create test rig for antennas
- 2- Far field characterization of microwave radiators
- 3- Develop testing software
- 4- Develop processing software
- 5- Define a user's manual for the test rig

1.2. Requirements and Specifications

The requirements for the testing rig are the following:

- It can be used repeatedly within tolerance, with similar results.
- It should be a transportable rig.
- It must give accurate results when used.
- It shall be versatile enough to withstand different types of antennas.

The specifications of this project are:

- The stand of the rig holds a precise stepper motor that rotates, enabling to characterize a 360° radiation pattern of the DUT.
- The processing software allows a real time reading of the results.
- Results can be displayed using different NWAs, i.e. ZVA24, ZVL6, E5071B, etc.
- Estimate gain directivity using the generalized Friis equation model.

1.3. Methods and Procedures

For the whole duration of the thesis, most of the work has been done in the RF laboratory at the IMTEK facilities, under the supervision of Taimur Aftab. All the programming and building has been done there. Some tests were also conducted in the laboratory, but the main ones were done in the warehouse.

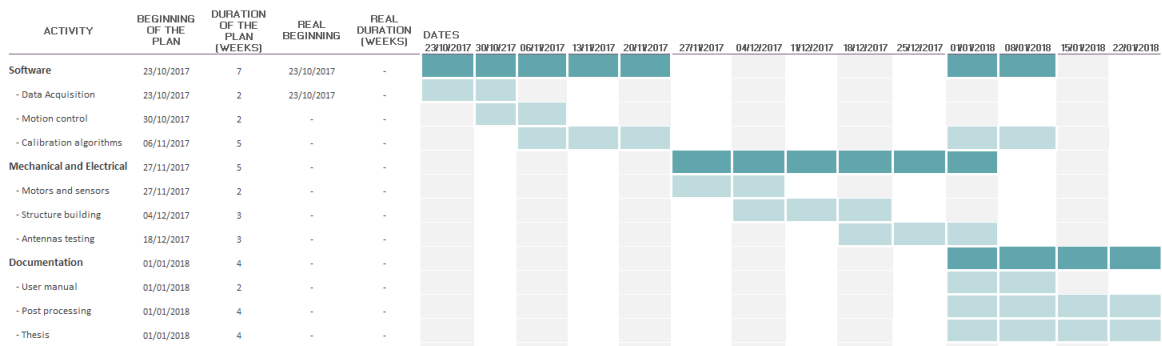
Different software has been used during the thesis for the different parts, such as MATLAB (motor programming, processing...), SolidWorks (3D pieces design), Ultimaker Cura (3D printing), LabView (antenna testing) or XMind (organization purposes).

1.4. Work Plan

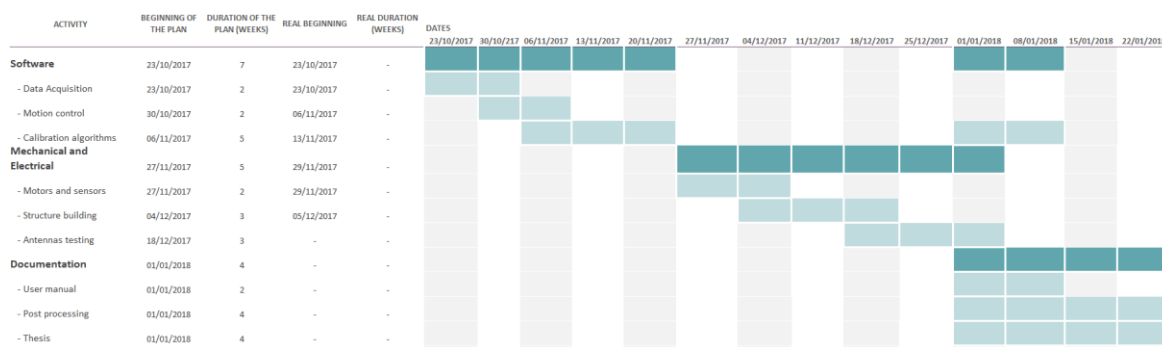
The work plan consists of the following work packages (WP):

- WP1: Software
- WP2: Mechanical and electrical
- WP3: Documentation
-

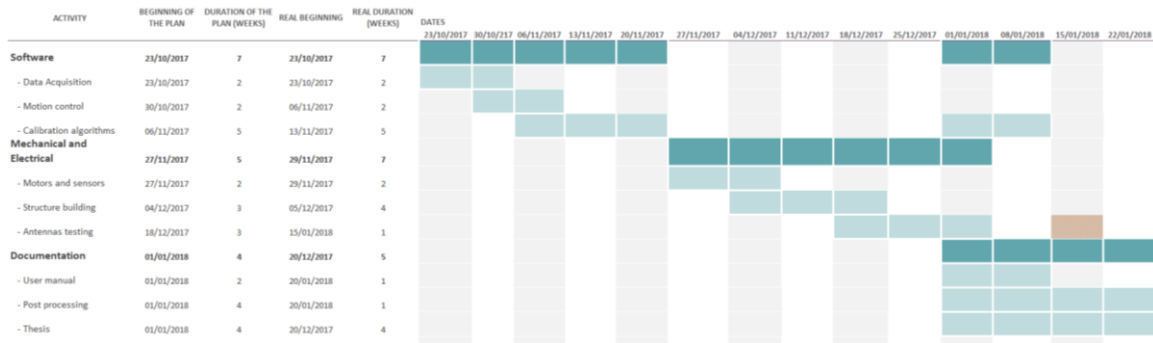
Together with the WPs, the Gantt diagram is also defined. Throughout the project it has changed several times due to incidences and delays, with the following results:



a)



b)



c)

Figure 1.1: Gantt Diagram representation throughout the project: a) Work Plan diagram, b) Critical Review diagram, c) Final Report diagram

1.5. Incidences and Modifications

Some incidences have occurred during the project, such as:

- Multiple 3D printing of pieces due to design flaws, misalignments, thermal issues or delamination
- Learning how to use SolidWorks for the first time.
- Problems with SolidWorks license.
- Delay in the programming of the stepper motor.
- Delay in the mechanical part due to imperial/metric differences in components (American/European measurement systems).

Because of the incidences listed above, and other external factors, the work plan has suffered from some modifications as well. In general, the work plan has been delayed and some things were done differently in order to finish on time, always trying to maintain the original idea. For example, the number of sensors incorporated to the rig is lower than expected, and the number of tests carried out at the end has also been lower.

2. State of the art of the technology used or applied in this thesis

2.1. Anechoic Chambers

An anechoic chamber is a room designed to completely absorb reflections of either sound or electromagnetic waves. They are also often isolated from waves entering from their surroundings. This combination means that a person or detector exclusively hears direct sounds (no reverberant sounds), in effect simulating being inside an infinitely large room.

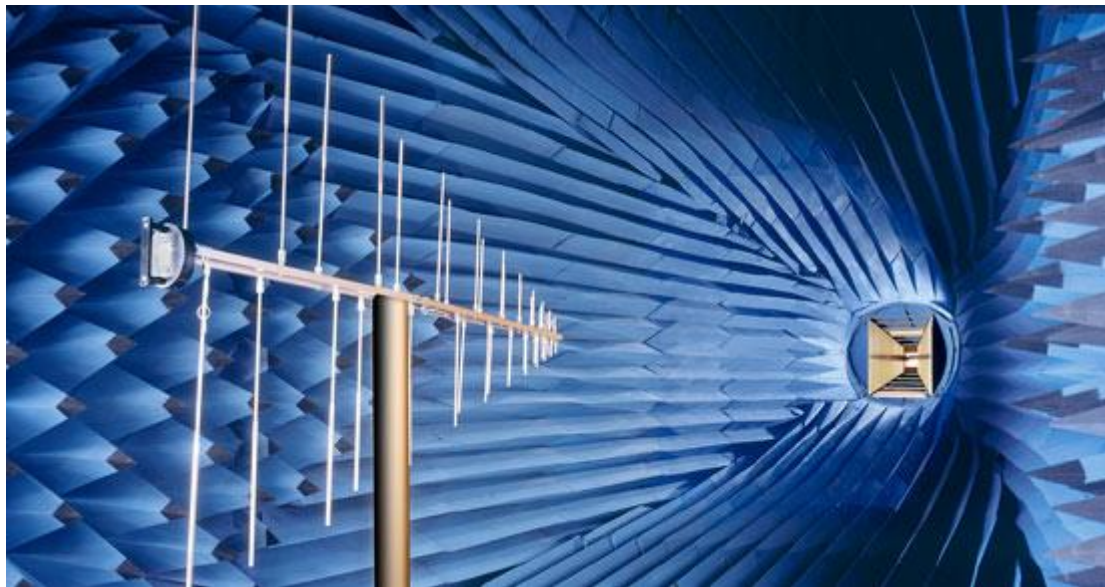


Figure 2.1: Anechoic chamber testing [1]

They were initially exclusively used to refer to acoustic anechoic chambers. Recently, the term has been extended to RF anechoic chambers, which eliminate reflection and external noise caused by electromagnetic waves.

Anechoic chambers range from small compartments the size of household microwave ovens to ones as large as aircraft hangars. The size of the chamber depends on the size of the objects and frequency ranges being tested.

There are 2 types of anechoic chambers: full and semi-anechoic chambers. A Fully Anechoic Room (FAR) is an anechoic chamber that has a substantial covering of anechoic material on the floor to effectively remove the ground reflection associated with a semi-anechoic chamber. Without a ground reflection, it no longer becomes necessary to sweep the receive antenna height, which can simplify testing procedures and result in shorter radiated emission test times.

For this project, it was not possible to test the antennas in an anechoic chamber due to the lack of one. However, the tests were conducted in a warehouse, big enough to simulate the effect of an anechoic chamber.

2.1.1. Radio-Absorbent Material (RAM)

RAM is designed and shaped to absorb incident RF radiation as effectively as possible. The more effective the RAM, the lower the resulting level of reflected RF radiation. Many measurements in electromagnetic compatibility and antenna radiation patterns require that spurious signals arising from the test set-up, including reflections, are negligible to avoid the risk of causing measurement errors and ambiguities.

In addition to the acoustic chambers, the anechoic radiofrequency chambers are enclosures with a metal shielding on their walls, emulating a Faraday cage. The chambers are lined with material designed for the absorption of electromagnetic waves (different from the material used to absorb acoustic waves) in order to isolate the chamber from any type of external influence and simulate free space conditions inside. These chambers have multiple applications in the field of telecommunications, such as measuring the specific absorption rate (SAR) of mobile terminals, or the design and characterization of radiant elements such as antennas and dipoles.

2.1.2. Electromagnetic Compatibility

Electromagnetic compatibility (EMC) is the branch of electrical engineering concerned with the unintentional generation, propagation and reception of electromagnetic energy which may cause unwanted effects such as electromagnetic interference (EMI) or even physical damage in operational equipment. The goal of EMC is the correct operation of different equipment in a common electromagnetic environment.

EMC pursues three main classes of issue. First, it studies the unwanted emissions and the countermeasures which may be taken in order to reduce such emissions. The second class, susceptibility, is the tendency of electrical equipment, referred to as the victim, to malfunction or break down in the presence of unwanted emissions, which are known as Radio Frequency Interferences (RFI). Immunity is the opposite of susceptibility, being the ability of equipment to function correctly in the presence of RFI, with the discipline of "hardening" equipment being known equally as susceptibility or immunity. A third class studied is coupling, which is the mechanism by which emitted interferences reach the victim.

While EMI is a *phenomenon* - the radiation emitted and its effects, EMC is an equipment *characteristic* or *property* - not to behave unacceptably in the EMI environment.

EMC ensures the correct operation, in the same electromagnetic environment, of different equipment items which use or respond to electromagnetic phenomena, and the avoidance of any interference effects. Another way of saying this is that EMC is the control of EMI so that unwanted effects are prevented.

In our case, as mentioned before, we are not able to perform the tests in an EMI free space. However, the warehouse where the tests take place is big enough to consider that EMC is achieved.

2.2. Applications

We can find applications of this particular area in different studies and projects:

2.2.1. Wireless Patch Antennas

The department of Mechanical and Aerospace Engineering, from the University of Texas in Arlington, have conducted a study called "*Wireless interrogation of passive antenna*

sensors” [1]. This paper presents a wireless method to remotely interrogate a dual-frequency antenna sensor. An interrogation horn antenna was used to irradiate the antenna sensor with a linear chirp microwave signal.

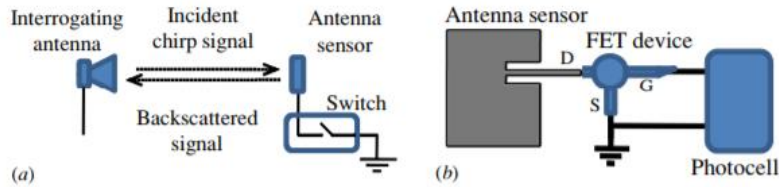


Figure 2.2: Wireless interrogation of the antenna sensor based on antenna backscattering: (a) antenna impedance switching; (b) implementation of light-activated RF switching [1]

2.2.2. Chip-based RFID

In a recent publication from the IEEE Sensors Journal, on the topic “RFID-Based Sensors for Zero-Power Autonomous Wireless Sensor Networks” [2], they talk about chip-based and chipless RFID sensors and their applications. Radio frequency identification (RFID) technology has enabled a new class of low cost, wireless zero-power sensors, which open up applications in highly wide and distributed RFID-enabled sensing, which were previously not feasible with wired or battery powered wireless sensor nodes. This paper provides a review of RFID sensing techniques utilizing chip-based and chipless RFID principles, and presents a variety of implementations of RFID-based sensors, which can be used to detect strain, temperature, water quality, touch, and gas.

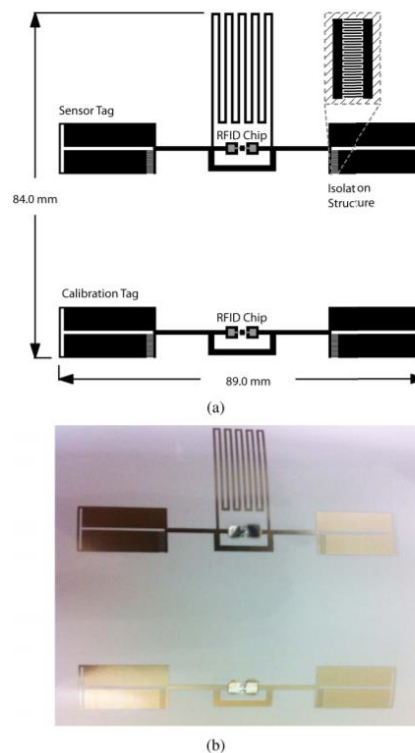


Figure 2.3: a) Design of the RFID chip-based touch sensor, b) inkjet printed RFID touch sensor prototype [2]

2.2.3. Retroreflectors Wireless Passive Sensing

Another example of application of this field can be found in a recent thesis called “*Numerical Modelling and Investigation of Isolated Dielectric Resonators for Wireless Passive Sensors*” [3], conducted at the Albert-Ludwigs University in Freiburg.

Numerous applications in automotive, aerospace and process industries require operation in severe conditions and harsh environments. Sensing solutions to monitor critical parameters in these applications are necessary in order to increase the systems lifetime or to reduce power consumption. These sensors must be small, robust and exhibit low manufacturing costs. Dielectric resonators based wireless passive sensors are potential candidates for such applications because they do not require any battery and can be interrogated without any physical connection to the reader electronics. These sensors measure the environmental parameters based on the change it causes to the dielectric-air boundary, subsequently leading to a shift in the resonance frequency of the resonator.

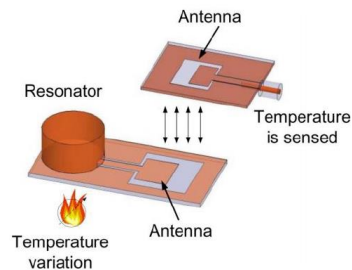


Figure 2.4: Wireless temperature sensing using DR with a separately coupled antenna [3]

The isolated dielectric resonator goes one step ahead as it allows external radiation with adequate far-field coupling, such that the need to use any external antenna or a conducting surface is avoided. The thesis document [3] thus focuses on the investigation of such isolated dielectric resonators for wireless passive sensing, where the resonator itself works both as a far-field antenna and as a sensor.

2.2.4. Urban Search and Rescue Antennas

At the School of Biomedical Engineering, in the Fourth Military Medical University in Xi’an (China), it is being developed a rescue system based in antennas, under the topic “*Wavelet Based Human Target Detection in Complex Ruins Using a Low Center Frequency UWB Radar*” [4].

Due to the complexity of ruin scenes in the post-disaster search and rescue operations, the Ultra-Wideband (UWB) echo signal reflected from the human target is often contaminated by the clutters and noises from the surrounding environment, which makes it difficult to extract the chest-wall micro-motion information that indicating the presence of human target, causing misjudgment and leakage. The paper proposes a novel feature extraction method based on wavelet transform to conquer the challenge.

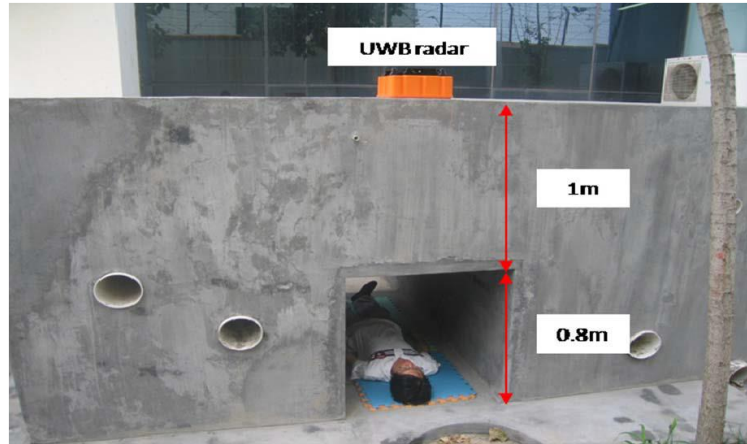


Figure 2.5: Testing set for USAR [4]

3. Methodology

3.1. Mathematical modelling

3.1.1. Link Budget

The *Link Budget* is a calculation of all the gains and losses from the transmitter, through the medium, to the receiver in a telecommunication system. The gains include antenna gains, transmission power and amplification in the receiver. Losses include attenuation within the transmitter and receiver, as well as the attenuation of the communication channel. Generally speaking, the *Link Budget* can be described as follows:

$$\text{Received Power (dB)} = \text{Transmitted Power (dBm)} + \text{Gains (dB)} - \text{Losses (dB)}$$

If you look at the gains and losses in detail, you will see the following formula:

$$P_{RX} = P_{TX} + G_{TX} - L_{TX} - L_{FS} - L_M + G_{RX} - L_{RX} \quad (3.1)$$

In this case:

P_{RX} : Received power (dBm)

P_{TX} : Transmitted power (dBm)

G_{TX} : Transmitter antenna gain (dB)

L_{TX} : Transmitter losses (cable, connectors...) (dB)

L_{FS} : Channel losses (i.e. free-space losses) (dB)

L_M : Other losses (fading margin, mismatches...) (dB)

G_{RX} : Receiver antenna gain (dB)

L_{RX} : Receiver losses (cable, connectors...) (dB)

The term Rx stands for *receiver mode* and the term Tx stands for *transmitter mode*. The highest losses result from the term L_{FS} , which describes the underlying channel model. In the case of free-space propagation, the path loss is calculated as follows:

$$L_{FS} = \left(\frac{4\pi r}{\lambda}\right)^2 \quad (3.2)$$

In simplified terms, the term can be expressed in dB form as follows:

$$L_{FS} = 32.4 + 20\text{Log}(r) + 20\text{Log}(f) \quad (3.3)$$

The units of r and f are kilometers and MHz, respectively. If r is specified in meters, the constant must be changed from 32.4 to -27.55. If the transmitter and receiver are located near the ground, multipath propagation by reflections is possible. The free-space model is therefore only suitable to a limited extent. In this case, a more accurate calculation is shown in section 3.1.3, taking into account multipath propagation.

3.1.2. Antennas

An antenna serves as transmitter and receiver of electromagnetic waves in free space. An antenna that acts as a transmitter converts a conducted electromagnetic wave into a free-space wave. On the other hand, a receiving antenna converts a free-space wave back into a conducted electromagnetic wave. Antennas can be characterised by their

radiation fields. In the following, the calculations are carried out under the assumption of a large distance to the antenna, which simplifies the radiation fields. With an isotropic omnidirectional radiator, the power P_S supplied to the antenna is emitted uniformly in all spatial directions. The radiant power density S_i at distance r results after [5] in:

$$\vec{S}_i(r) = \frac{P_S}{4\pi r^2} \vec{e}_r \quad (3.4)$$

The efficiency in an antenna transmission applies for the main beam direction of the antenna, this means for the direction in which the directional function is maximum. Furthermore, the “*Equivalent Isotropically Radiated Power*” P_{EIRP} is introduced:

$$P_{EIRP} = GP_S \quad (3.5)$$

It indicates the power supplied to an isotropic spherical radiator which is required to produce the same radiant power density in this direction.

A further variable is used for a receiver antenna. The maximum effective antenna aperture A_e [6] as a function of wavelength λ results in:

$$A_e = \left(\frac{\lambda^2}{4\pi}\right) G = \left(\frac{\lambda^2}{4\pi}\right) D\eta = A_w\eta \quad (3.6)$$

The antenna aperture A_e is the product of the active antenna surface A_e and efficiency η and is used to calculate the power P_E :

$$P_E = A_e S \quad (3.7)$$

3.1.3. Friis Equation

In order to be able to estimate the range of a radio system, the power coupled into the receiver system must be examined. In the following, the power $P_{s,SR}$ coupled into a receiving system according to equation 3.7 is considered. If we substitute A_e and S from equation 3.6 we obtain

$$P_E = A_e S = \left(\frac{\lambda}{4\pi r}\right)^2 G_E P_{s,SR} \quad (3.8)$$

The index “*SR*” means that it is the power of a spherical radiator. Therefore, the following applies:

$$P_{s,SR} = P_{EIRP} \quad (3.9)$$

Using equation 3.5, the following Friis equation is obtained after [6]:

$$P_E = \left(\frac{\lambda}{4\pi r}\right)^2 G_E G_S P_S \quad (3.10)$$

It describes the correlation between the parameters from the transmitter and receiver and the range of an electromagnetic wave in the free space. The parameters are:

λ = wavelength

r = radial distance from transmitter antenna

P_E = received power

P_S = transmitted power

G_E = gain of receiver antenna

G_S = gain of transmitter antenna

By including the equation

$$\lambda f = c \tag{3.11}$$

With λ = wavelength

f = frequency

c = speed of light

The Friis equation can also be reformulated as:

$$r = \frac{c}{4\pi f} \sqrt{\frac{P_S G_S G_E}{P_E}} \tag{3.12}$$

If a constant transmitting power P_S and minimum receiving power P_E is assumed, the range r_{max} of a communication system is given as an anti-proportional dependence on the frequency:

$$r_{max} \propto \frac{1}{f} \tag{3.13}$$

A halving of the frequency should thus lead to a doubling of the range if the antenna is increased in equal measure. In practice, however, these theoretical antennas are limited because factors such as multipath propagation reduce the maximum range. The electromagnetic waves are reflected by objects and the ground, and thus overlap. The representation of the multipath propagation over a flat surface is shown in Figure 3.1:

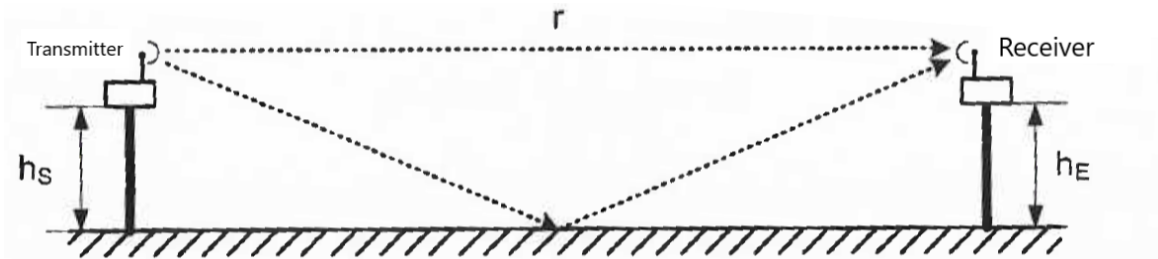


Figure 3.1: Two-way propagation by ground reflections from transmitter (S) to receiver (E)

If the height of the antennas is much smaller than the distance r between them ($r \gg h_S, h_E$), thus, assuming an average gain for the transmitter and the receiver, the following applies after [5] and [7]:

$$P_E = 2 \left(\frac{\lambda}{4\pi r} \right)^2 \left[1 - D \cos \left(\frac{4\pi h_S h_E}{\lambda r} \right) \right] G_E G_S P_S \tag{3.14}$$

Ground reflections lead to points of constructive interference at which a higher power than 3.10 is to be expected. However, there will be points where the waves will overlap destructively, and the signal will be weakened. Additionally, the parameter D is introduced, which takes into account the ground condition during the reflection.

For the propagation of electromagnetic waves within a building, the path loss after [7] can be expressed according to the *ITU Model for Indoor Attenuation*:

$$L_{dB} = 20 \log(f) + N \log(d) + L_{floor}(n) - 28dB \tag{3.15}$$

With f : frequency in MHz

d : distance in m (>1m)

N : distance loss coefficient (≈ 30)

$L_{floor}(n)$: wall losses

n : Number of floors between transmitter and receiver

3.2. Software

For the software development, several programs were used. The more significant ones for this project were MATLAB, SolidWorks and LabView. Currently, the IMTEK department already has a LabView code for the antenna testing, but not a MATLAB one. The idea of using MATLAB is to be able to implement all the functions (data acquisition, motion control, testing and processing) into a single one, from which the whole process will be controlled. Due to lack of time, it was not possible to put them all together, so the actual testing of the antennas was done with LabView. Nevertheless, all MATLAB functions work separately and will be implemented in the future into one.

3.2.1. MATLAB

MATLAB has been the main programming tool for this project. It has been used for data acquisition (DAQ), motion control and processing.

- DAQ:

First, the parameters of frequency sweep and number of points used for the measurements are set. After the desired NWA is selected (ZVL, E5071B...) and initialized, the NWA takes the measurements and uses the raw data to create a complex matrix with the results. Then, it displays them in real time in the NWA's screen. Later, these data will be processed.

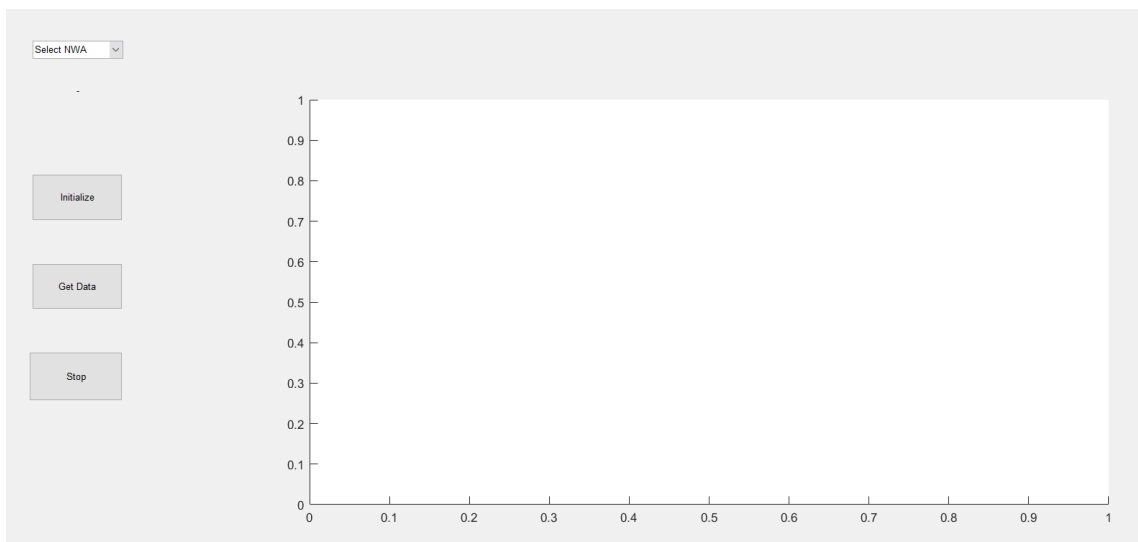


Figure 3.2: Data extractor uninitialized

- Motion control:

For the motion control, the controller used was the TCM-1110 stepRocker, a module for stepper motors with a wide and simple programming capacity. The controller commands are intuitive and easy to use, and allows the user to

manipulate the stepper motor depending on what they need. In this case, only a few commands are used. Since the project's goal is to characterize the radiation pattern of an antenna, the stepper motor needs to turn right or left at a certain speed, for a certain number of degrees to make it possible. As seen in Figure 3.3, the motor can rotate to any of its sides, while updating its current position (in degrees) in real time, until it reaches the final point.

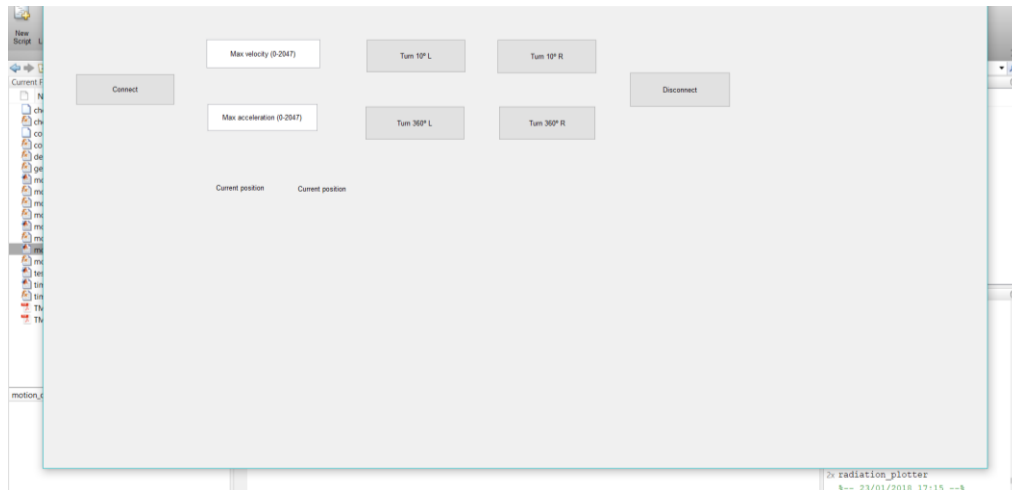


Figure 3.3: Motion control commands

Besides the stepper motor, an encoder (Yumo A6B2) has been added in order to help with the motion control, with parameters such as the number of turns, speed or position of the motor.

- Post processing

The post processing of the information takes care of the .csv files generated when taking measurements. The information that these files contain is as follows:

- Measurement time
- Shaft angle
- Frequency sweep
- Parameters 1 and 2 (S_{11} , S_{21} , S_{31} ...), real and imaginary part

With this information, a group of radiation patterns is generated, each one at a different frequency.

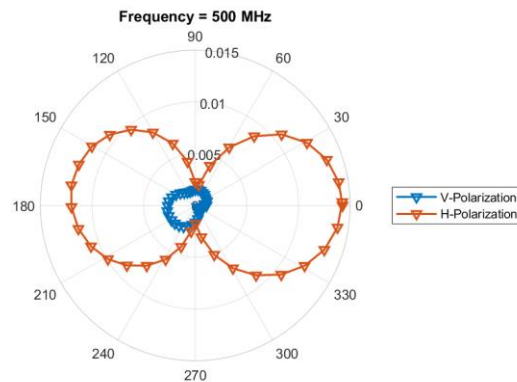
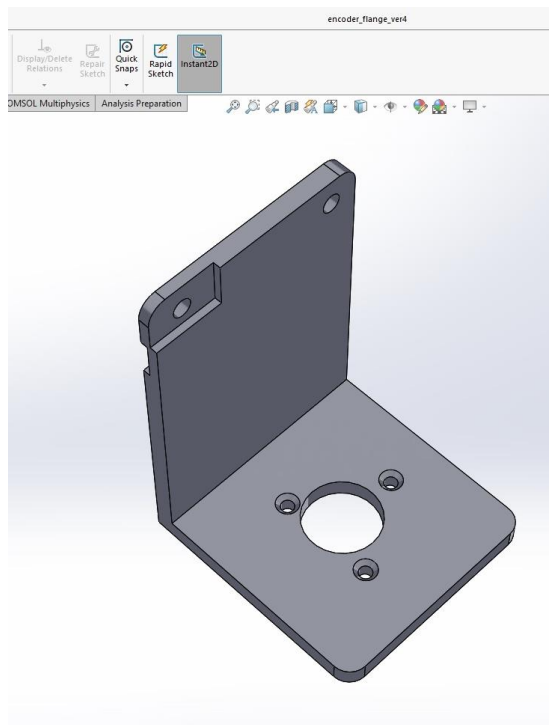


Figure 3.4: Example of radiation pattern of dipole at 500MHz

3.2.2. SolidWorks and Ultimaker Cura

SolidWorks is a solid modelling computer-aided design (CAD) and computer-aided engineering (CAE) program. It allows to model parts and assemblies and extract from them both technical drawings and other information necessary for production. It is a program that works based on new CAD modeling techniques.

For this project, SolidWorks has been used to design 3D pieces, necessary for the correct functioning of the stepper motor. Some of the pieces can be seen in the next figures:

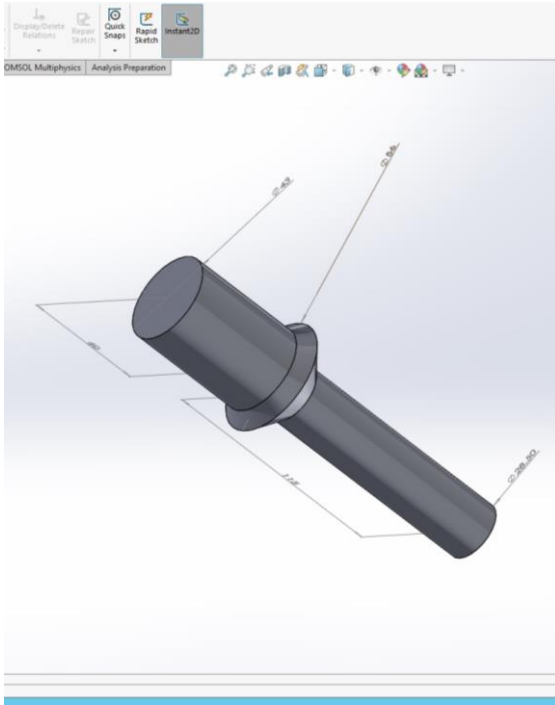


a)



b)

Figure 3.5: a) first design of encoder holder, b) printed final piece



a)

b)

Figure 3.6: a) design of shaft holder, b) printed shaft holder

After the piece is modelled in SolidWorks, it is printed with the program Ultimaker Cura. Cura is a 3D printer slicing application, which is the preferred slicer software for Ultimaker 3D printers, although it can be used with other printers as well.

With this application, the user can choose between a whole variety of settings for the printing, such as quality, wall thickness, infill or speed, as seen in the next set of figures:

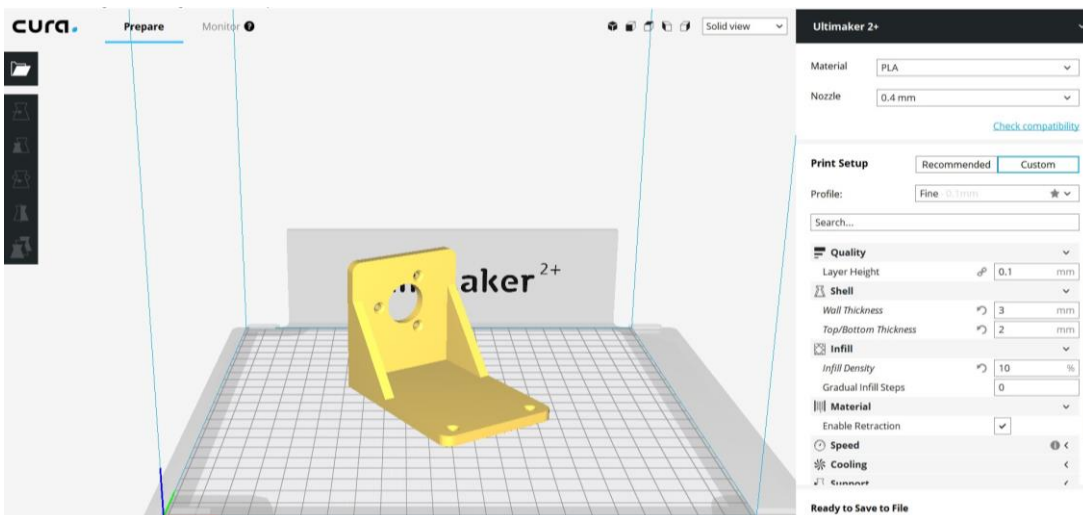


Figure 3.7: Ultimaker design of encoder holder

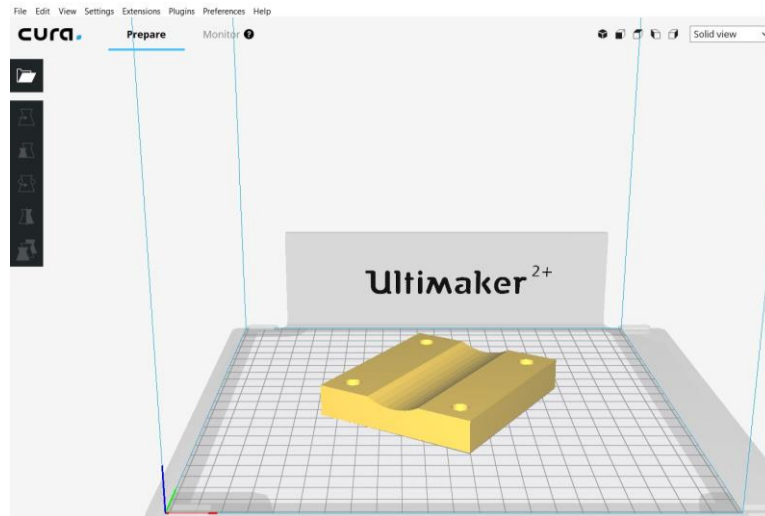


Figure 3.8: Ultimaker design of holding piece

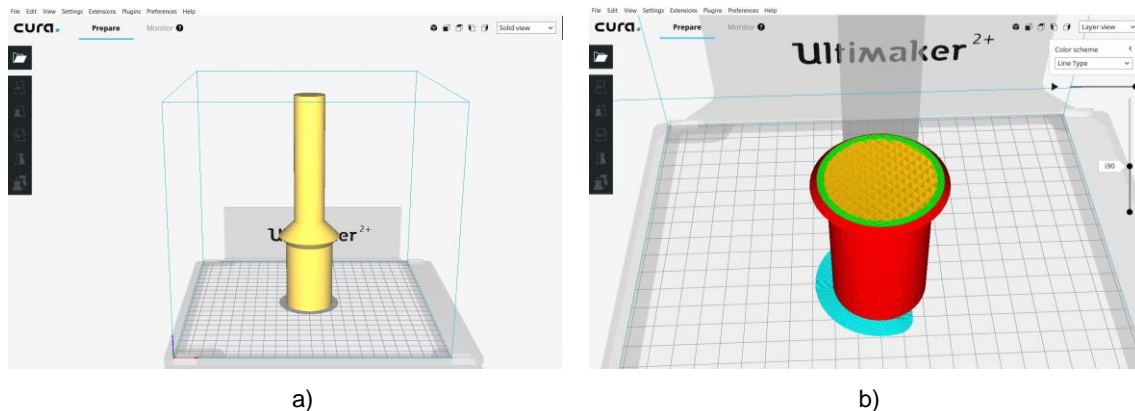


Figure 3.9: a) Ultimaker design of shaft holder, b) different layers of shaft holder

3.2.3. LabView

LabView was used for the testing of the antennas. The advantage of using LabView is that the IMTEK department already had a code for this purpose. It only needed some adjustments for this specific project and it was ready to use. Otherwise, to implement it on MATLAB and check its correct functioning would have taken too long.

A more detailed explanation of its functioning will be explained later, in 3.4.2.

3.3. Hardware

For the hardware part, two main aspects were considered. First, the stepper motor used for the rotation of the antenna. The second one, the stand structure where everything is put together.

3.3.1. Stepper motor

A stepper motor is an electromechanical device which converts electrical pulses into discrete mechanical movements. The shaft of a stepper motor rotates in discrete steps when electrical command pulses are applied to it in the proper sequence [8].

The main advantages of using a stepper motor are:

- Precise positioning and repeatability of movement.
- Excellent response to starting/stopping/reversing commands.
- It is possible to achieve very low speed synchronous rotation with a load that is directly coupled to the shaft.
- Different speeds can be set for the rotation.

For this project, the stepper motor that has been used already belonged to the IMTEK department, which means it was not necessary to purchase or build a new one. However, what needed to be done was the programming of it, together with some adjustments and 3D printing. As mentioned in 3.2.1, MATLAB was used to program it. In order to do so, the controller used for this motor was the TCM-1110 stepRocker. In addition to the controller, an encoder was added to the stepper motor.

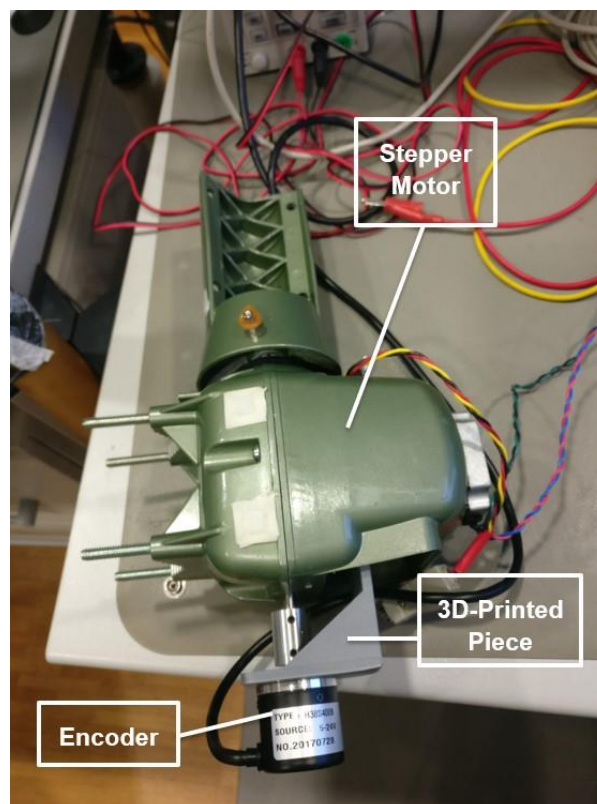


Figure 3.10: Stepper motor parts

The motor rotates with a resolution of 200 steps/revolution, each step with a resolution of 256 microsteps/step.

The motor by itself was not enough to attach to the stand structure, and could not hold the encoder, which was necessary for its functioning. Because of that, several parts needed to be 3D-printed. Some of those parts can be seen in 3.2.2. For example, a

support structure to connect the inside plate of the motor to the encoder, or a shaft piece placed on top of the motor.



Figure 3.11: Stepper motor inside gears

3.3.2. Stand Structure

The stand structure consists of a triangular base with a pole (pole A) standing on it. At the same time, leaning on pole A there is another pole (pole B) with the stepper motor attached to it. The shaft of the motor must be aligned perfectly with the center of pole B, so that there are no misalignments when it rotates. A 3D part was printed with the exact diameter to solve that.

On top of pole B there is the antenna holder, where the DUT is placed for the tests.

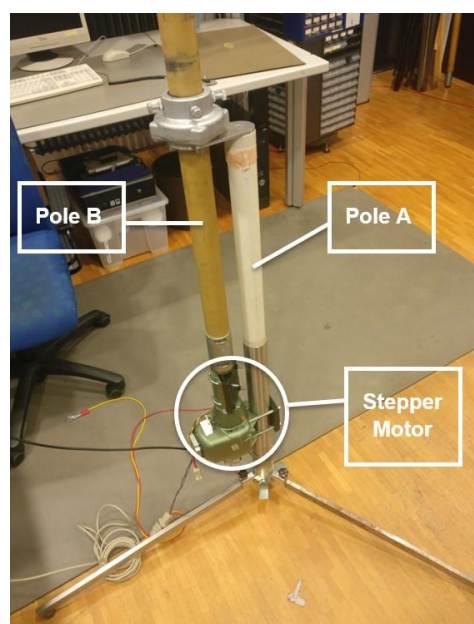


Figure 3.12: Stand structure for stepper motor and DUT

3.4. User Manual

3.4.1. Antenna Stand Set-Up

In the next figures, an example of the set-up for the antenna stand can be seen. This set-up was done in the RF laboratory for the first tests, and the final set-up is shown in 4.1.

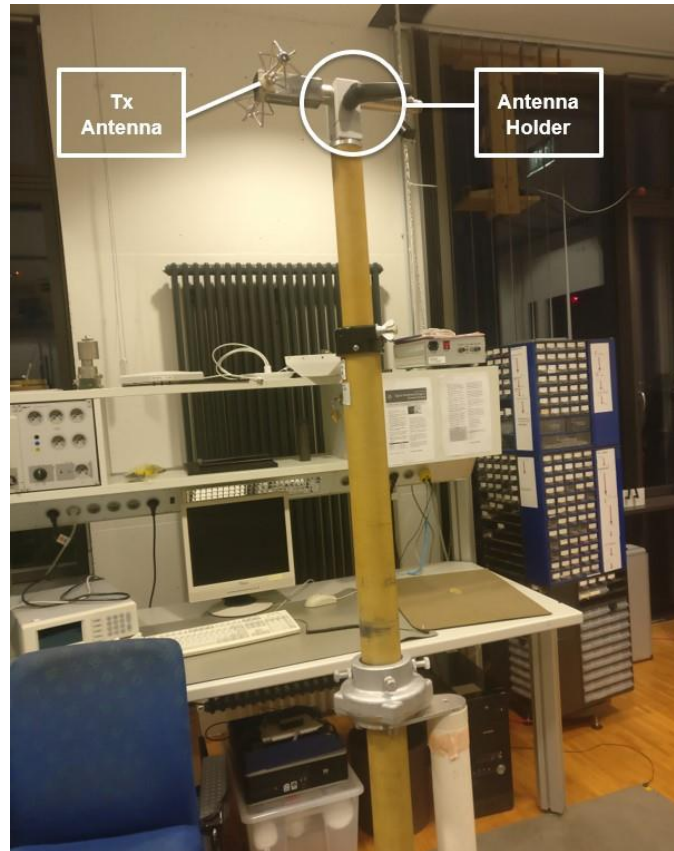


Figure 3.13: DUT and antenna stand

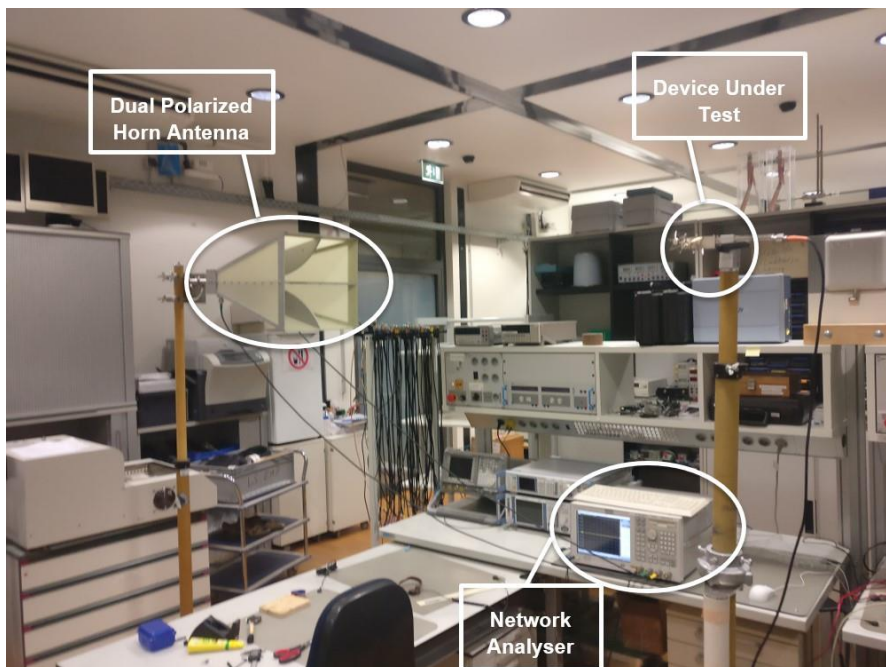


Figure 3.14: Test set-up example, done in the RF laboratory

Ideally, the antennas should be at the same height, pointing directly at each other. The DUT should be connected to *Port 1* of the NWA, and the other antenna to *Port 2* (H-polarization) and *Port 3* (V-polarization).

3.4.2. Parameters Set-Up and Measurement

After the antennas are placed in the correct position and all the connections are made (NWA, antennas, computer, power supply...), the set-up of the parameters is necessary. This is done with the LabView program explained in 3.4.2. When all the parameters are set, the program can run and start taking measurements.

As shown in Figure 3.15, the way it works is very simple. On the left side, the configuration screen, and on the right side the visualizing screen. The values seen here are the default settings, but can be changed depending on the user's needs.

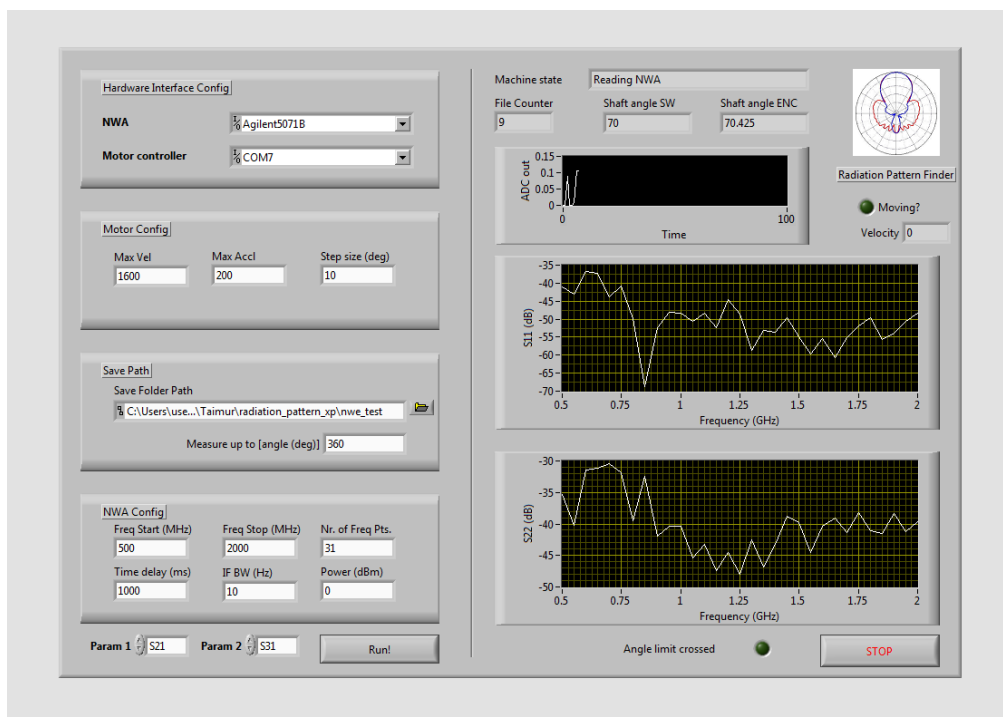


Figure 3.15: LabView screen for the antenna tests

In *Hardware Interface Config*, the NWA is chosen together with the motor controller port. In this specific case, the E5071B is being used, and the controller is connected to COM7.

Then, in *Motor Config*, the velocity, acceleration and step size of the stepper motor are selected. The step size represents how many degrees the antenna will rotate before stopping and taking the measurements.

In the section *Save Path*, there is the folder where the generated .csv files will be saved. Also, here the user sets the limit angle until which the antenna should rotate.

Later on, in *NWA Config* the parameters of the NWA are set. These parameters are: frequency start and stop, number of points between those frequencies, time delay, IF bandwidth and transmitted power.

Besides all that, there are 2 other parameters that can be set: *Param 1* and *Param 2*. These are the parameters measured by the NWA and saved for its later processing. The user can decide which of those parameters to measure, i.e. S_{11} , S_{21} , S_{31} , etc.

On the right side of the screen, the top part represents the state of the rotation, where two important parameters can be seen. They are: *Shaft angle SW* (software) and *Shaft angle ENC* (encoder). The first one is the angle (in degrees) that the stepper motor is supposed to be rotated with respect to the starting position, and the second one is the rotation angle that the encoder measures, the “real rotation”. If the difference is too big for the ongoing experiment, the user can see it and decide whether to start over or not.

Finally, when the antenna reaches its limit angle, it stops automatically. Throughout the whole experiment, the program generates a series of .csv files after each step, which will be processed later.

A visual representation of how the program works can be seen in Figure 3.16:

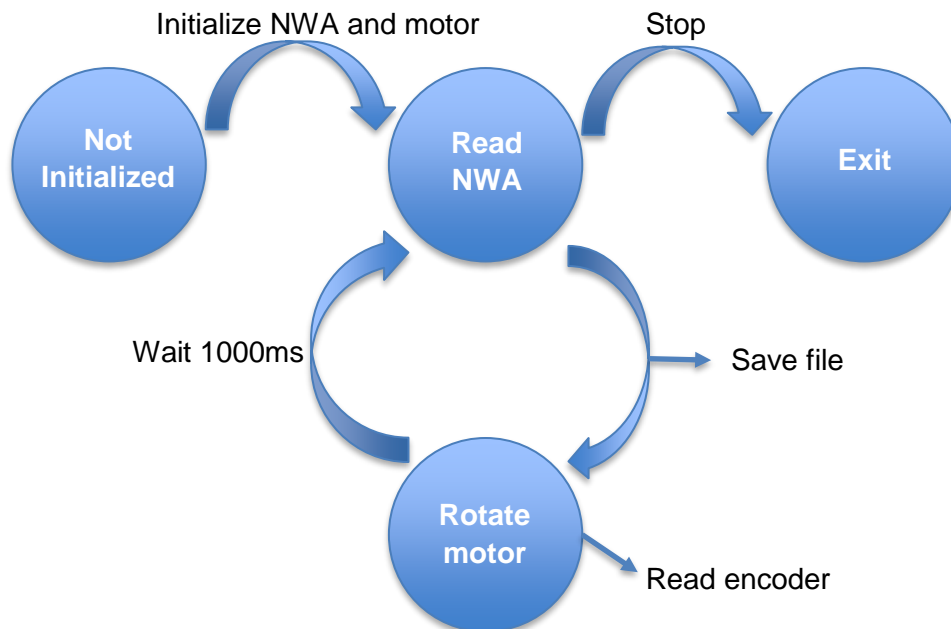


Figure 3.16: State diagram of the LabView program

4. Results

The results of this project can be divided into 2 sections: hardware and software performance. The hardware includes the mechanical performance of the testing rig that was built. The software results are the ones corresponding to the processing of the measurements.

4.1. Hardware Performance

The mechanical part of the project has worked out well, although some unplanned problems have come up when testing. The final set-up can be seen in Figure 4.1.

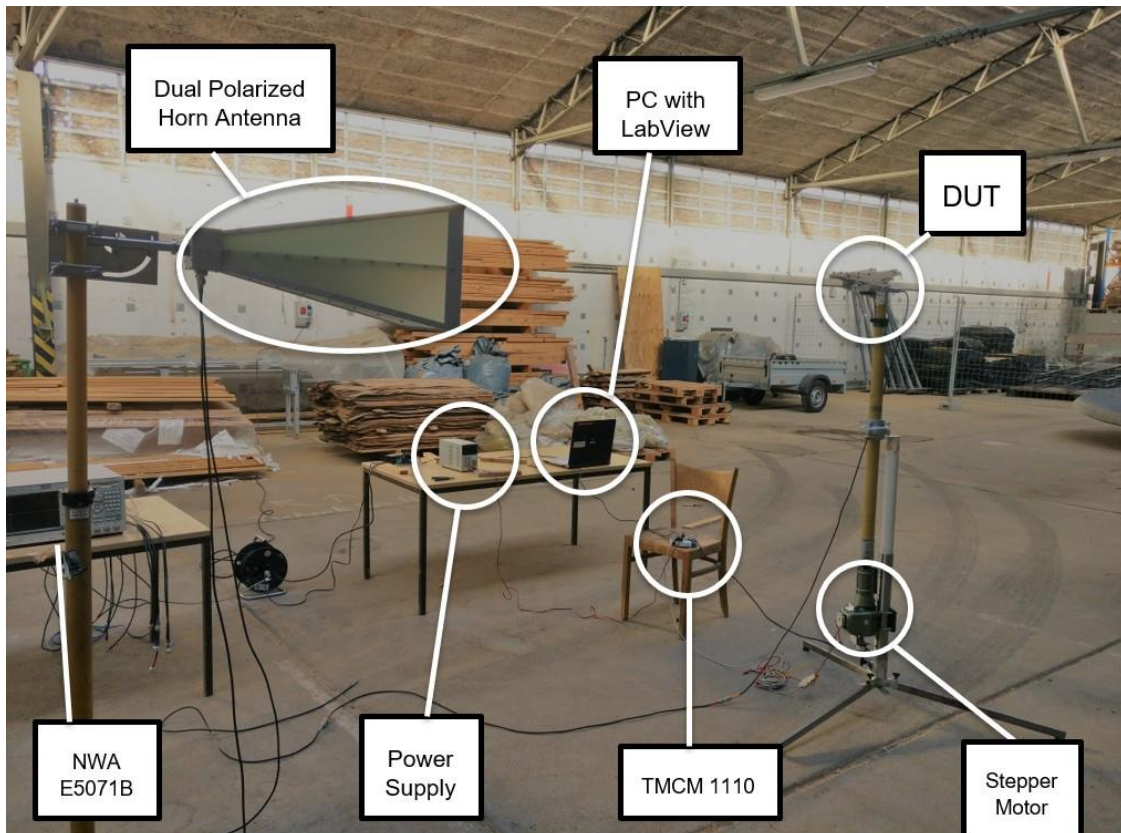


Figure 4.1: Final set-up for the experiments in the warehouse

The stepper motor has worked perfectly, there have been no problems with its functioning. The antenna holders on both sides have also worked well. The only problem with the mechanical part has been caused by the cables. In some of the tests the antenna has rotated 360°, and in others 720°. Due to the rotation of the antenna, the cable connecting the DUT and the NWA has been coiling around the pole, which was especially problematic with the 720° tests. The cable rolled around the pole causing strain, which lead to a misreading in some of the experiments. The antenna was supposed to rotate a certain angle in each step, but because of this tension it rotated less than it should have. In these cases, the experiment was performed again.

4.2. Software Performance

The software results of the different experiments have also been successful. As mentioned before, the lack of time has not allowed to conduct all the experiments wanted in this project. Nevertheless, the ones obtained are considered successful and set the base for future experiments.

The main idea of the data processing is to obtain the radiation pattern of the DUT. For that purpose, a double polarized horn antenna (see Figure 4.1) is set as the known device, and thanks to it, the DUT can be tested both in horizontal and vertical polarization. The LabView program saves a .csv file for each of the sweeping frequencies, and with the MATLAB processing software the radiation patterns for the different frequencies are generated.

Several antennas have been tested during the experiments. Following, the antennas are described and a representative radiation pattern of them is displayed. To illustrate the good functioning of the system, a radiation pattern has been added for each of the antennas, where the measuring frequency is out of range. Also, a representation of the vertical and horizontal polarization values S_{21} and S_{31} is shown for each antenna.

4.2.1. Dipole Antenna

Figure 4.3 shows the different radiation patterns of the dipole antenna. This dipole works in the frequency range 0.5-3 GHz. It was oriented horizontally when tested, that is why the radiation pattern shows a good response in the H-polarization, while in the V-polarization it is almost null.



Figure 4.2: Dipole antenna, 0.5-3GHz

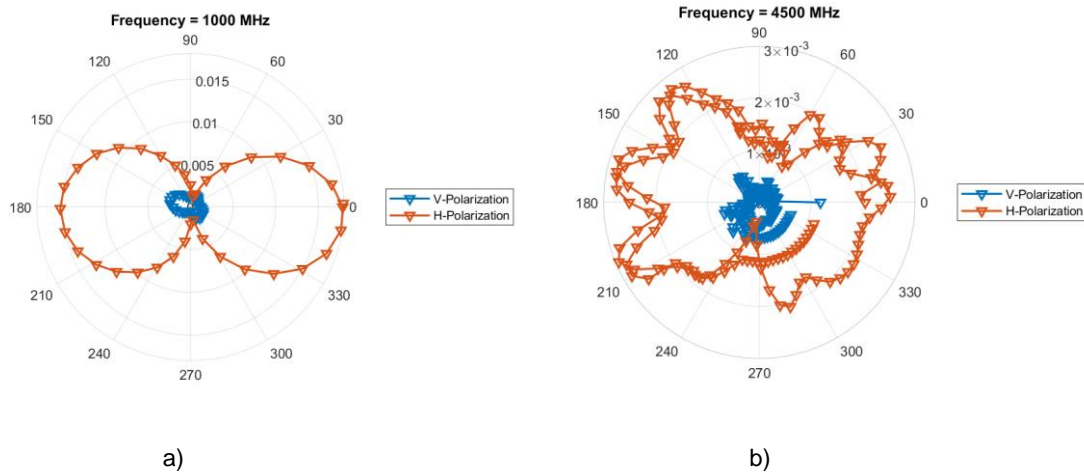


Figure 4.3: Radiation patterns of dipole; a) inside frequency range, b) outside frequency range

As it can be seen in 4.4, between the ranges 0.5-3GHz the dipole shows a good response, and out of that range the S_{21} and S_{31} values decrease.

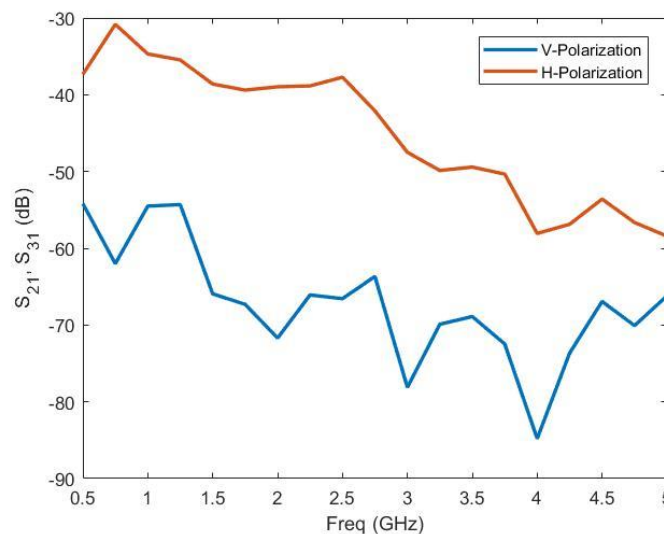


Figure 4.4: V- and H-Polarization values (dB) of the dipole for different frequencies

4.2.2. Hybrid PA-23R Antenna

The frequency range of this antenna is 1.24-1.32 GHz. As seen in the following Figures, when the frequency is in this range, the antenna has a high directivity in the V-polarization. When it goes out of the range, the secondary lobes start to grow, and the S_{21} magnitude also decreases.

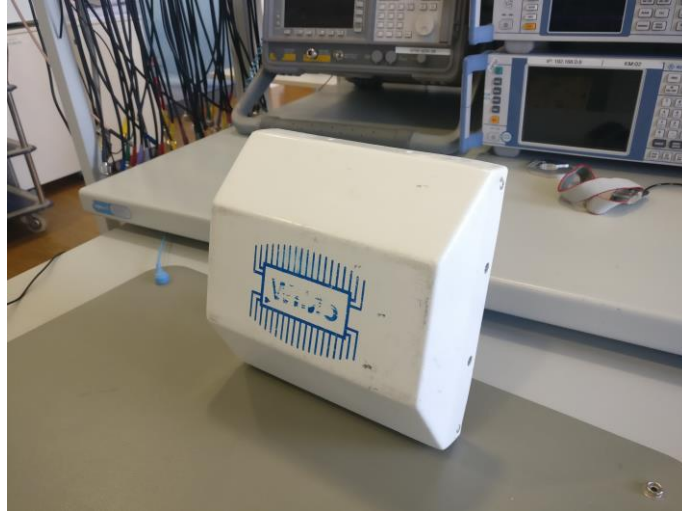
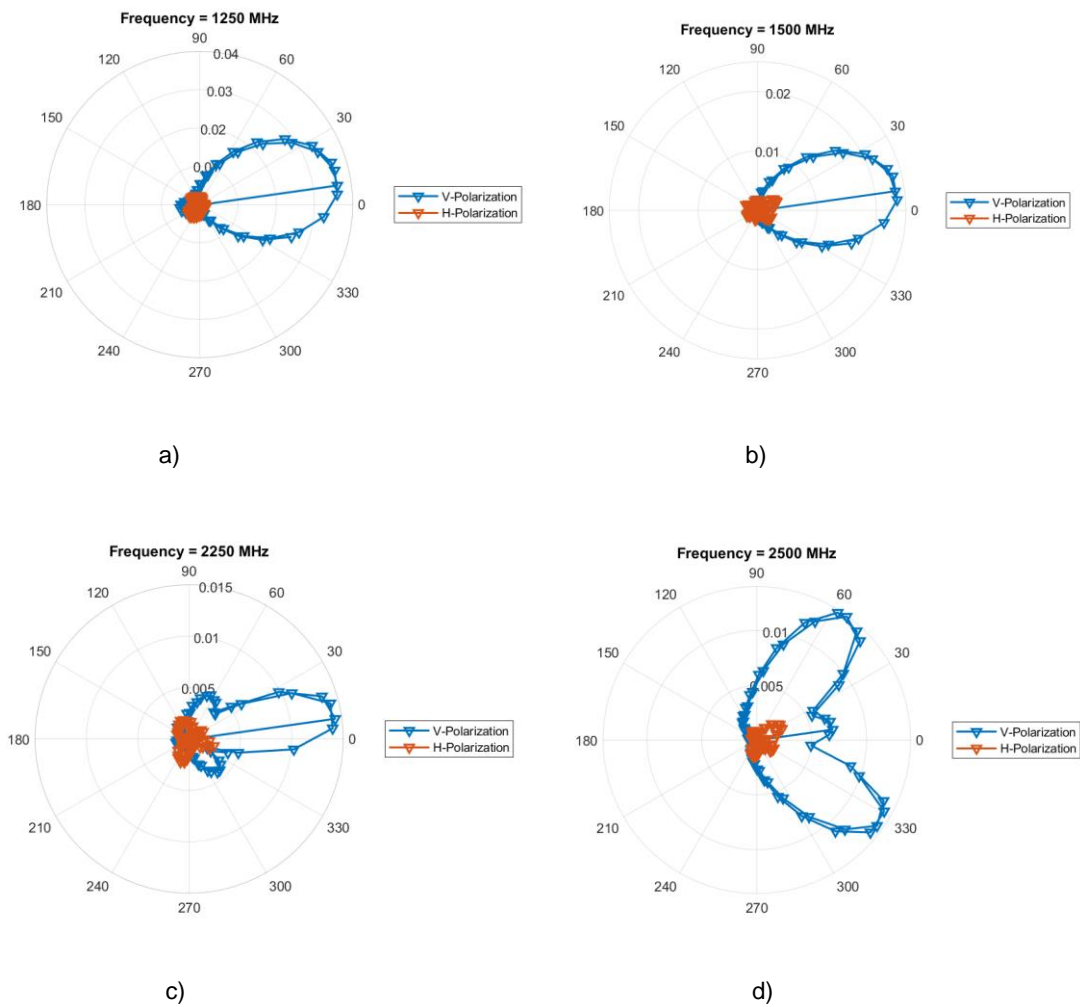


Figure 4.5: WiMo PA-23R antenna, 1.24-1.32GHz



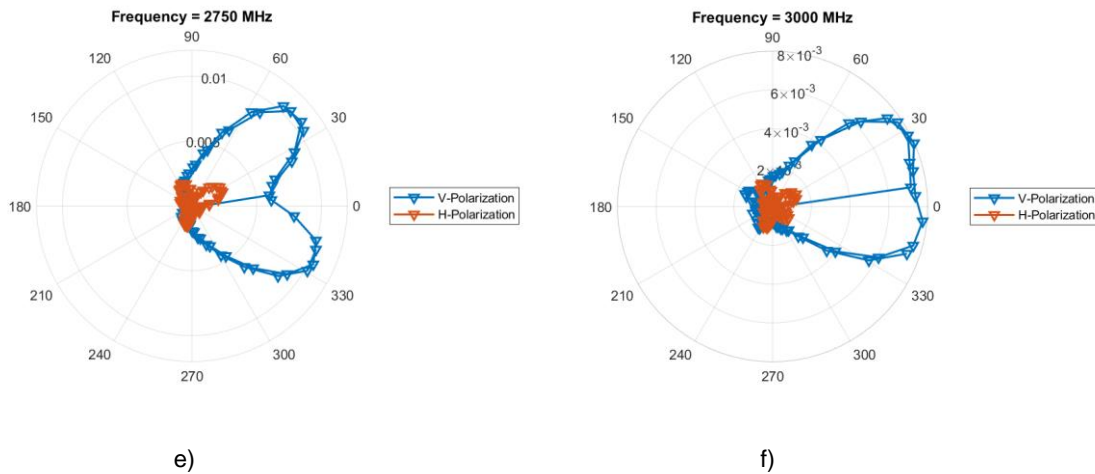


Figure 4.6: Radiation patterns of PA-23R antenna; a) and b) inside frequency range, c), d), e) and f) outside frequency range

Figure 4.7 shows the S_{21} and S_{31} values, with a peak at 1.25GHz, matching with the frequency range of the antenna and confirming its good functioning.

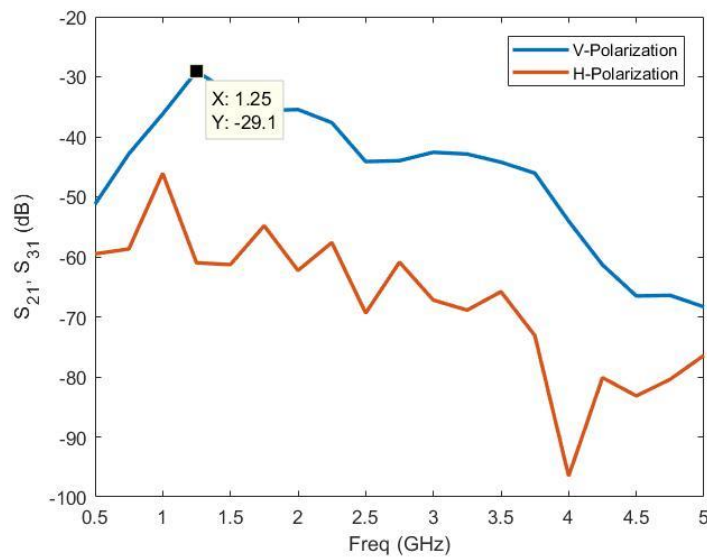


Figure 4.7: V- and H-Polarization values (dB) of the PA-23R antenna for different frequencies

4.2.3. 2.4GHz Flat Antenna

This antenna's frequency range is 2.3-2.5 GHz. Figure 4.8 shows its directivity in the H-polarization. In the next ones, it can be seen how it destabilizes when the frequency is not in the range.



Figure 4.8: Flat Antenna, 2.3-2.5GHz

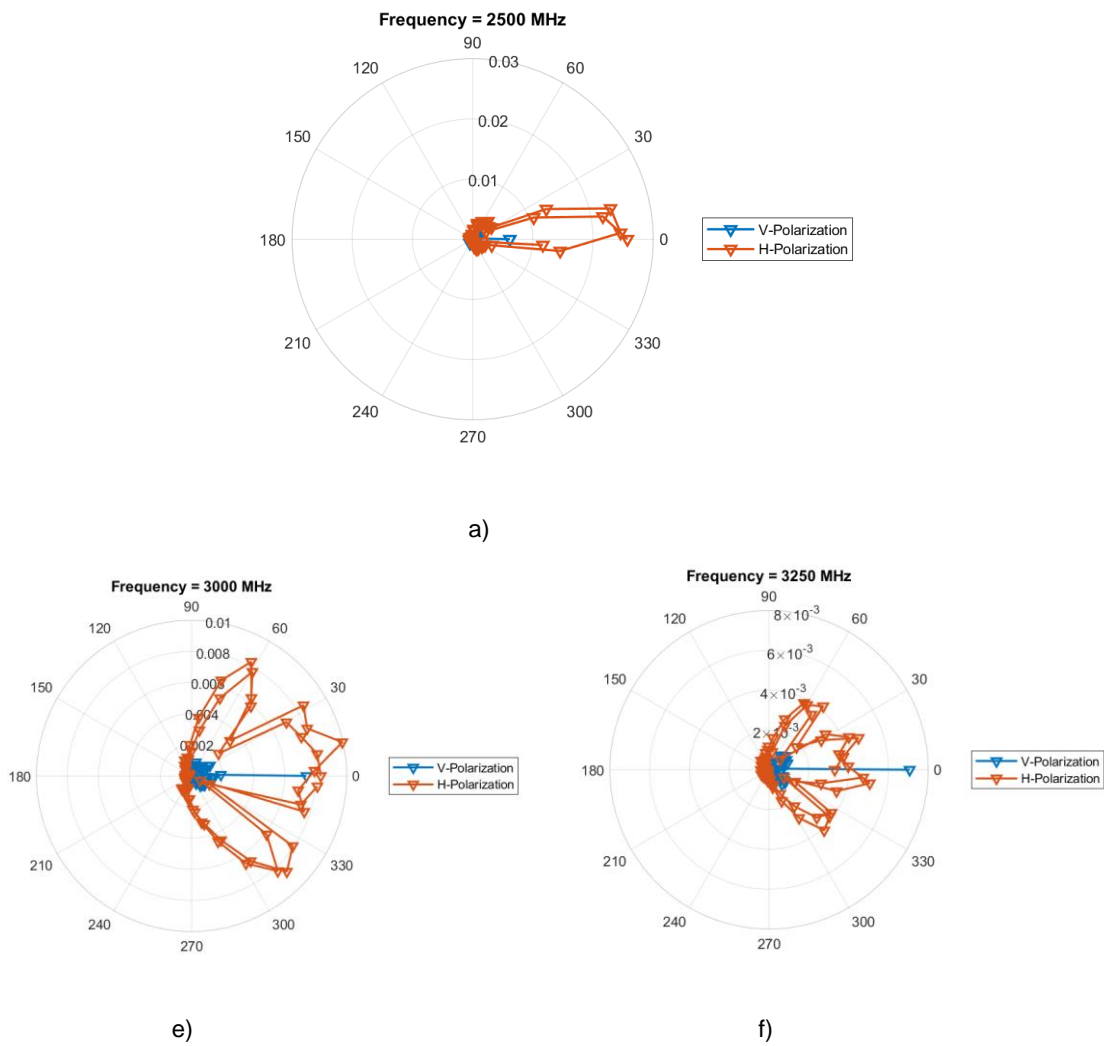


Figure 4.9: Radiation patterns of flat antenna; a) inside frequency range, b) and c) outside frequency range

In Figure 4.10, S_{21} and S_{31} are seen, with a peak at 2.5GHz, also matching the radiation pattern diagram.

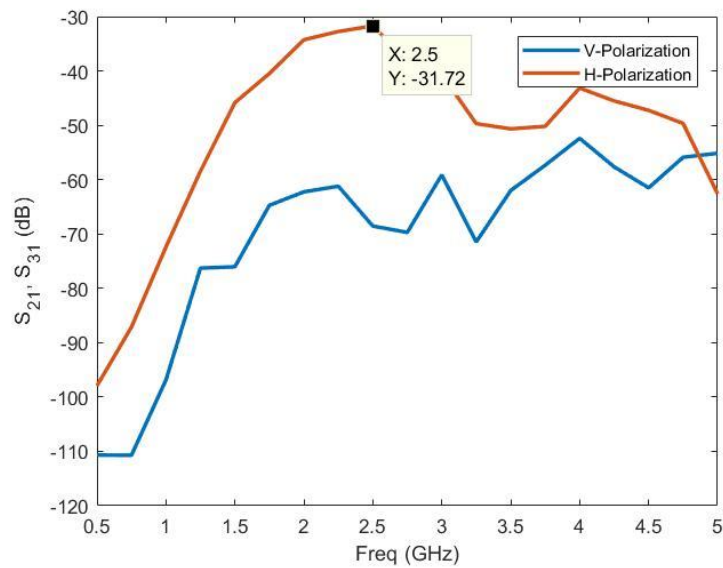


Figure 4.10: V- and H-Polarization values (dB) of the flat antenna for different frequencies

5. Budget

The budget for this project includes the following:

	Wage/hour	Hours	Cost
Junior engineer	8 €/h	30 h/week	3.840 €
Senior engineer	20 €/h	5 h/week	1.600 €
Photoelectric rotary encoder	-	-	21,50 €
Mechanical pieces	-	-	10 €
SolidWorks license	-	-	6.600 €
PLA printing material	-	-	30 €
3D printer Ultimaker 2+	-	-	1.895 €
TOTAL			16.080 €

In the first place, the hours dedicated by the student (Junior engineer) and the tutor (Senior engineer), with their respective wage/hour.

Besides these values, the most significant ones are the license of SolidWorks and the cost of the 3D printer. However, it was not necessary to buy them because the IMTEK department already owns both the license and the printer.

Finally, the cost of the materials bought for the project is also included, although it is very low compared to the rest of the budget.

6. Conclusions and future development

The main goal of this project was to build a testing rig for different types of antennas. The rig should also have a software that allows to set any desired parameters for the testing, as well as a processing software for the measurements. According to these premises, the main objective of the thesis has been achieved.

Most of the software and hardware were developed during the project. However, some of it was already existing at the beginning. The stepper motor and the stand for the antennas were already property of the IMTEK department. The LabView software was developed before this project, so with some modifications it was possible to use it here too. Thanks to this, it was possible to accelerate the process and finish on time.

Besides this, not all objectives were accomplished. Due to lack of time, some of the ideas that were thought at the beginning were not implemented. For example, the transportable trolley was not finally built, and the different sensors could not be incorporated.

In the end, also due to lack of time, only a few tests were performed in the warehouse. Some of them were done in the RF laboratory at the IMTEK facilities, where reflections and interferences can affect the measurements. Because of that, the only ones that have been taken into account are the ones carried out in the warehouse.

With more time to develop the project, some things could have been added to make the results better. As a future work, besides the above-mentioned characteristics, some features can also be incorporated to the system. To make sure that the antenna starts and finishes a complete round exactly at the same point, a laser can be added to have a visual idea of this and make adjustments. Another idea is that several clamps can be 3D-printed for different types of antennas and retroreflectors, depending on how they are positioned and the way to hold them. It is also important to have a box for the electronic components all together, so it is easier to move, and safer for the electronic parts.

As a conclusion, the results of the project have been satisfactory, although with more time to make it, more things could have been added to the final outcome. It still needs improvement and additional features, which will make it more reliable and efficient.

7. Bibliography

- [1] S. Deshmukh, and H. Huang. "Wireless interrogation of passive antenna sensors". IOP Publishing Ltd, January 2010.
- [2] B. S. Cook *et al.*, "RFID-Based Sensors for Zero-Power Autonomous Wireless Sensor Networks," in *IEEE Sensors Journal*, vol. 14, no. 8, pp. 2419-2431, Aug. 2014. DOI: 10.1109/JSEN.2013.2297436
- [3] Shah Hussain. "Numerical Modelling and Investigation of Isolated Dielectric Resonators for Wireless Passive Sensors". M.S. thesis, Department of Microsystems Engineering, Albert-Ludwigs University, Freiburg, Germany, 2016.
- [4] Qiang An *et al.*, "Wavelet Based human target detection in complex ruins using a low center frequency UWB radar," *2016 Progress in Electromagnetic Research Symposium (PIERS)*, Shanghai, 2016, pp. 1744-1747. DOI: 10.1109/PIERS.2016.7734777
- [5] F. Gustrau. *High-frequency technology - Basics of mobile communication technology*. Hanser, pp. 8-12, 2011.
- [6] J. Curty, M. Declercq, C. Dehollain, and N. Joehl. *Design and optimization of passive UHF RFID systems*. Springer-Verlag, 1. Edition, 2007.
- [7] J. Seybold. *Introduction to RF Propagation*. John Wiley & Sons, 1. Edition, 2005.
- [8] Engineering Content EC, 2015. "Stepper Motor". [Online] Available: <https://engineeringcontent.blogspot.de/2015/03/stepper-motor.html> [Accessed: 25 October 2018]

8. Appendices

8.1. Horn Antenna Specifications

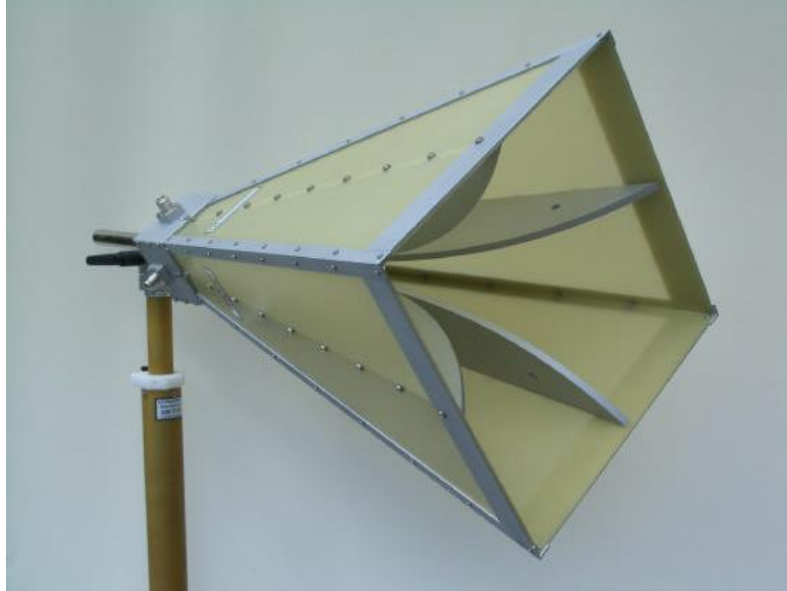


Figure 8.1: Double polarized horn antenna

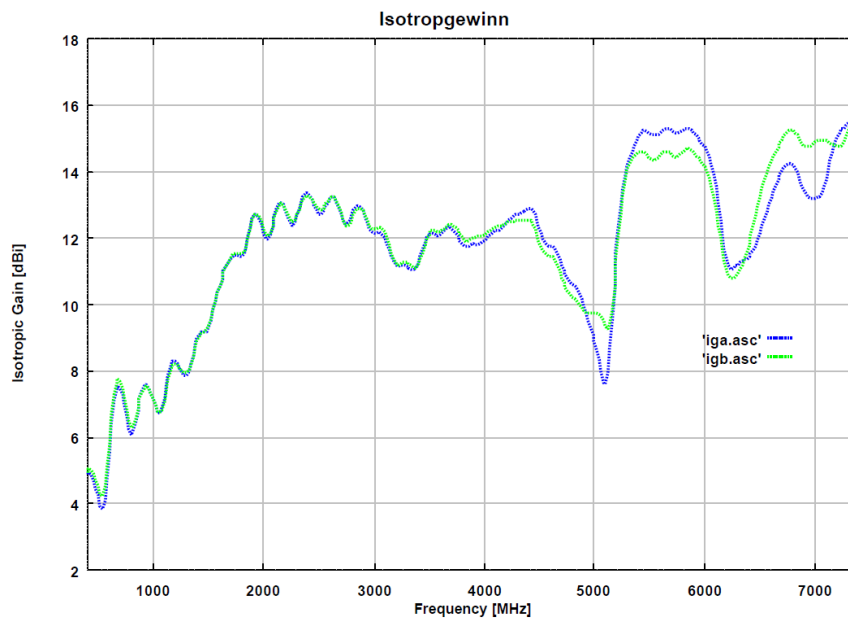


Figure 8.2: Isotropic gain for different frequencies

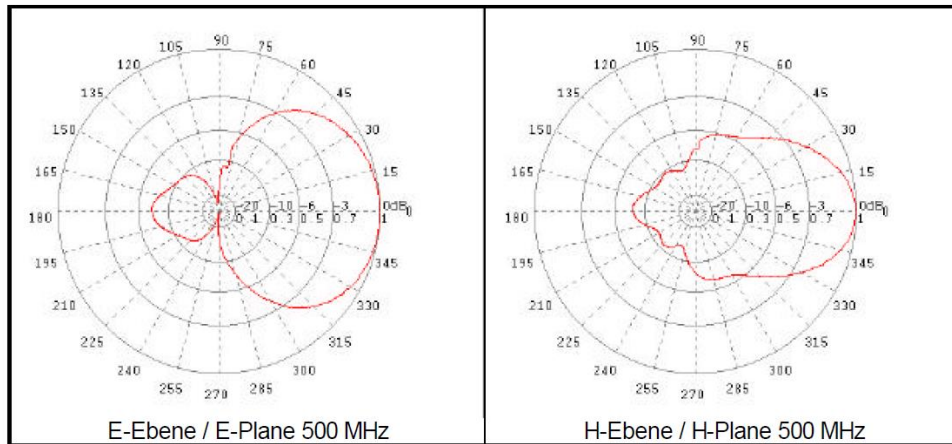


Figure 8.3: Radiation pattern for 500MHz, E-Plane and H-Plane

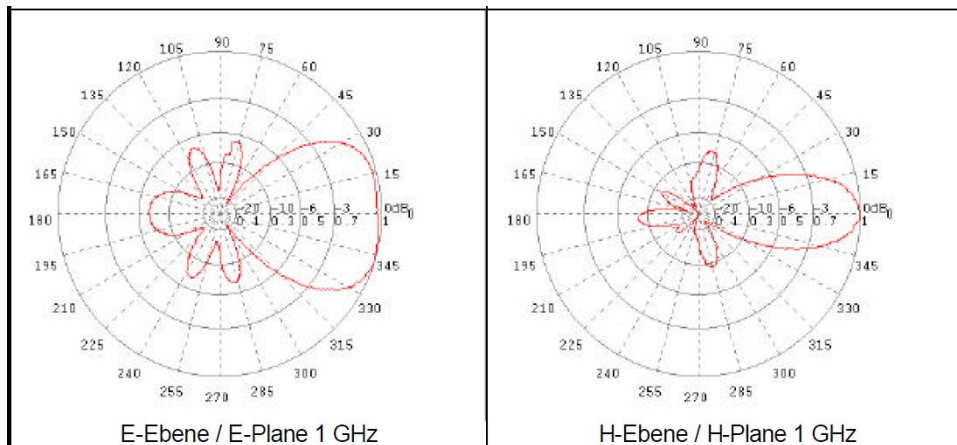


Figure 8.4: Radiation pattern for 1GHz, E-Plane and H-Plane

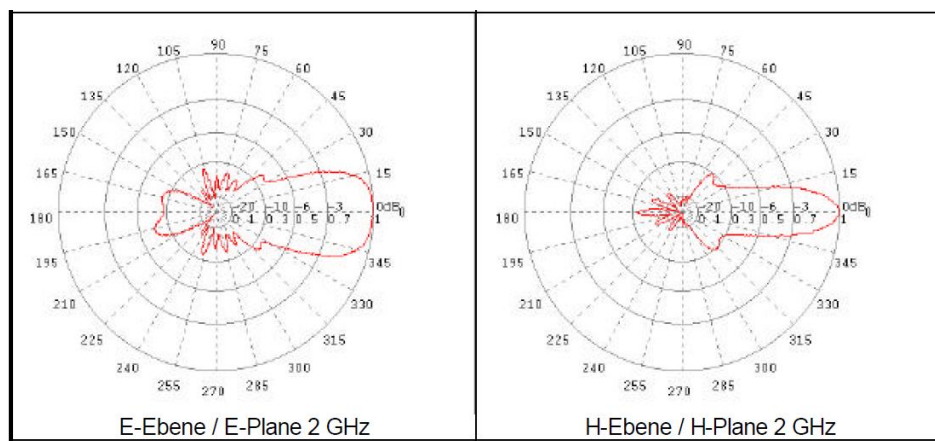


Figure 8.5: Radiation pattern for 2GHz, E-Plane and H-Plane

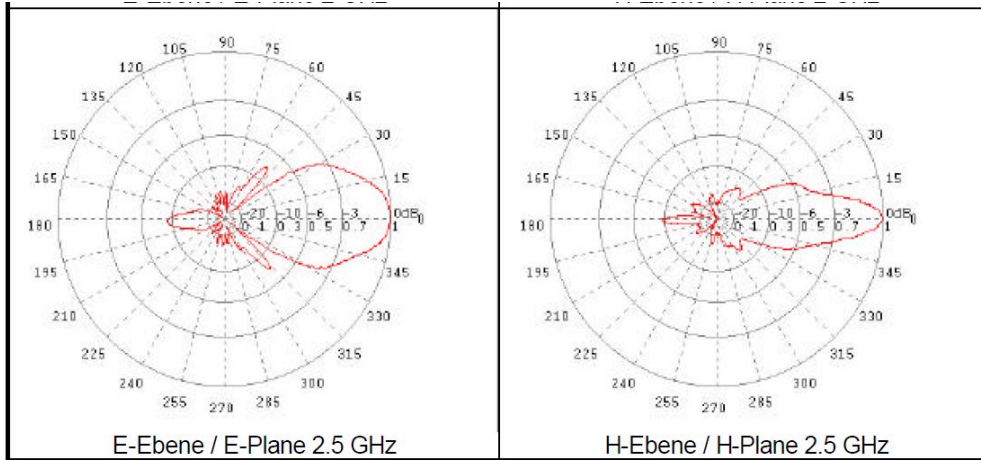


Figure 8.6: Radiation pattern for 2.5GHz, E-Plane and H-Plane

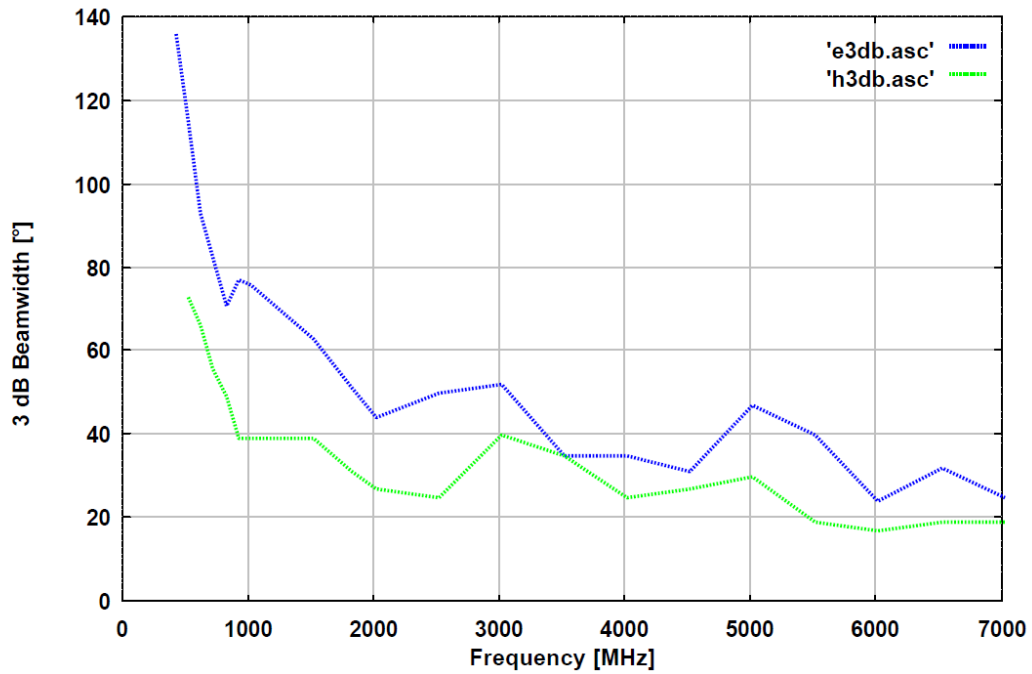


Figure 8.7: 3dB bandwidth at different frequencies

9. Glossary

CAD: Computer-Aided Design

CAE: Computer-Aided Engineering

DAQ: Data Acquisition

DR: Dielectric Resonator

DUT: Device Under Test

EMC: Electromagnetic Compatibility

EMI: Electromagnetic Interference

FAR: Fully Anechoic Room

IMTEK: Institut für Mikrosystemtechnik (Department of Microsystems Engineering)

NWA: Network Analyser

RAM: Radio-Absorbent Material

RF: Radio Frequency

RFI: Radio Frequency Interferences

RFID: Radio Frequency Identification

SAR: Specific Absorption Rate

SAW: Surface Acoustic Wave

UWB: Ultra-Wideband

WP: Work Package